High purity in HVPE method as an advantage used for controllable doping of GaN - influence of different dopants on electrical, optical, and structural properties of GaN crystals

unipress

GaN growth methods

HVPE

Growth rate > 100µm/h

T: 1045°C

p: ≤ 1 atm.

Ammonothermal

Growth rate: up to 10µm/h

T: 400-600°C

p: 1000-6000 atm.

Na-Flux

Growth rate: up to 50µm/h

T < 900°C

P < 100 atm.

Purity of HVPE-GaN

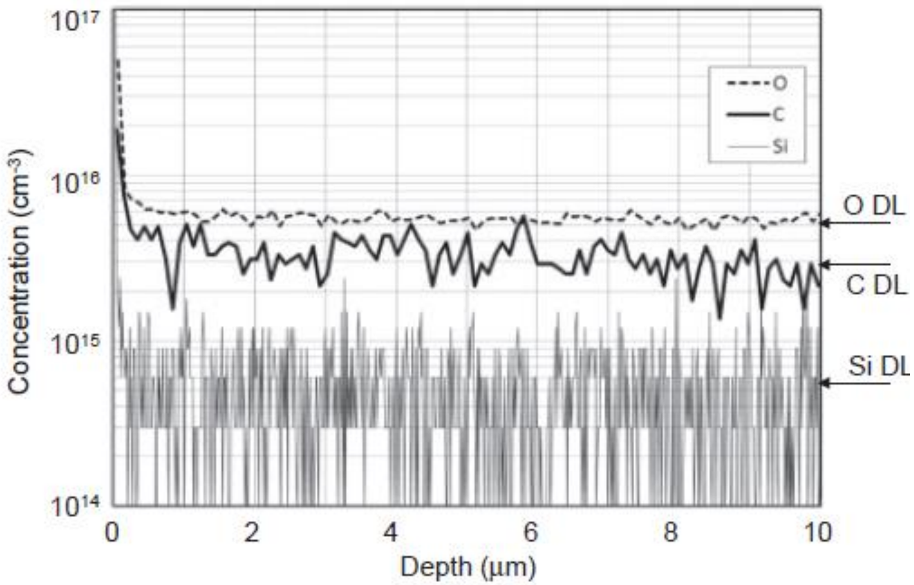

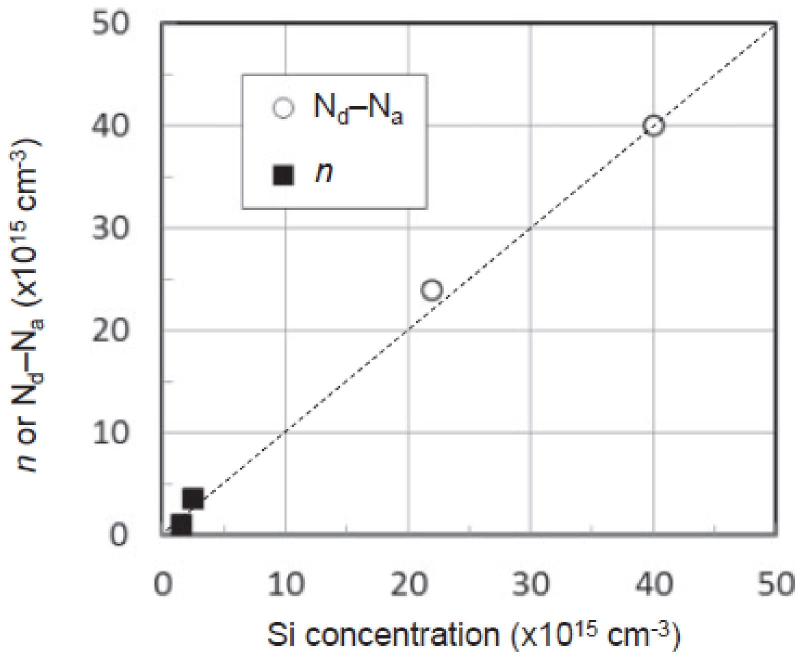

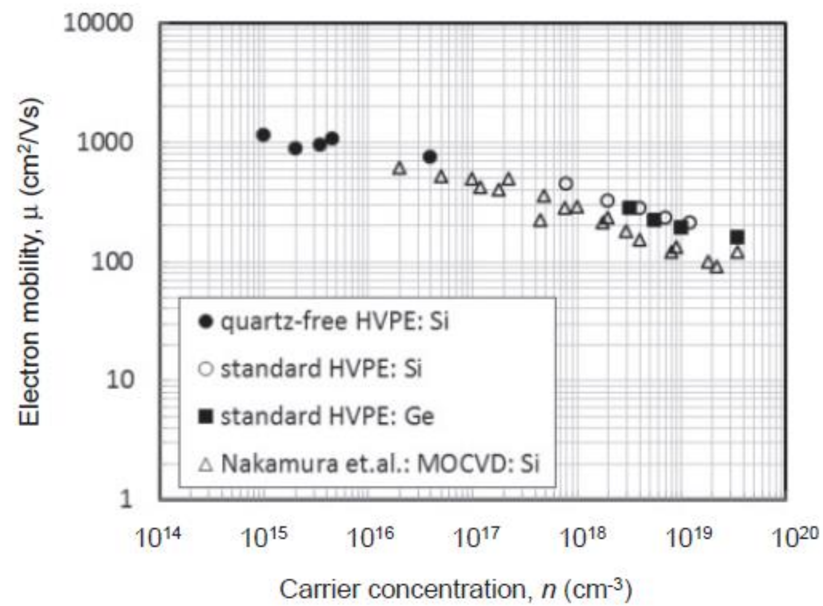

SCIOCS

H. Fujikura et al., Japanese Journal of Applied Physics 56, 085503 (2017)

HVPE method

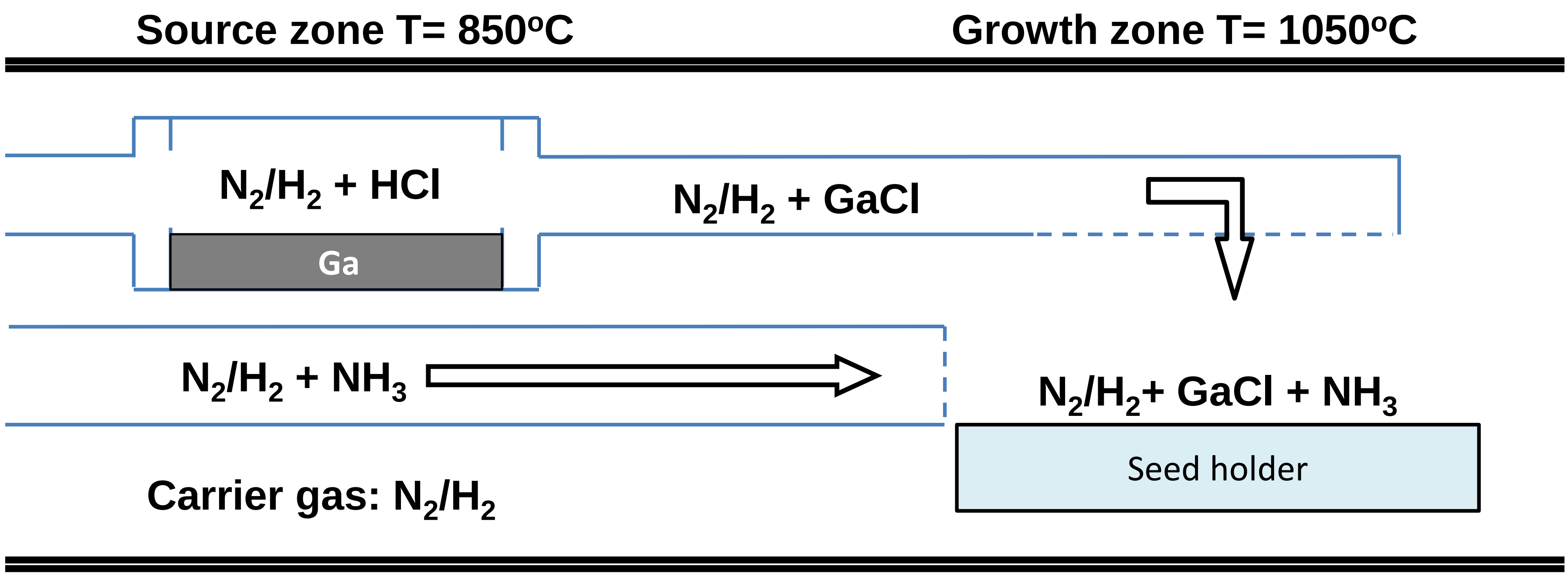

$$2HCl_{(g)} + 2Ga_{(l)} = 2GaCl_{(g)} + H_{2(g)}$$

$$GaCl_{(g)} + 2HCl_{(g)} = GaCl_{3(g)} + H_{2(g)}$$

$$GaCl_{(g)} + NH_{3(g)} = GaN_{(s)} + HCl_{(g)} + H_{2(g)}$$

Undoped HVPE-GaN

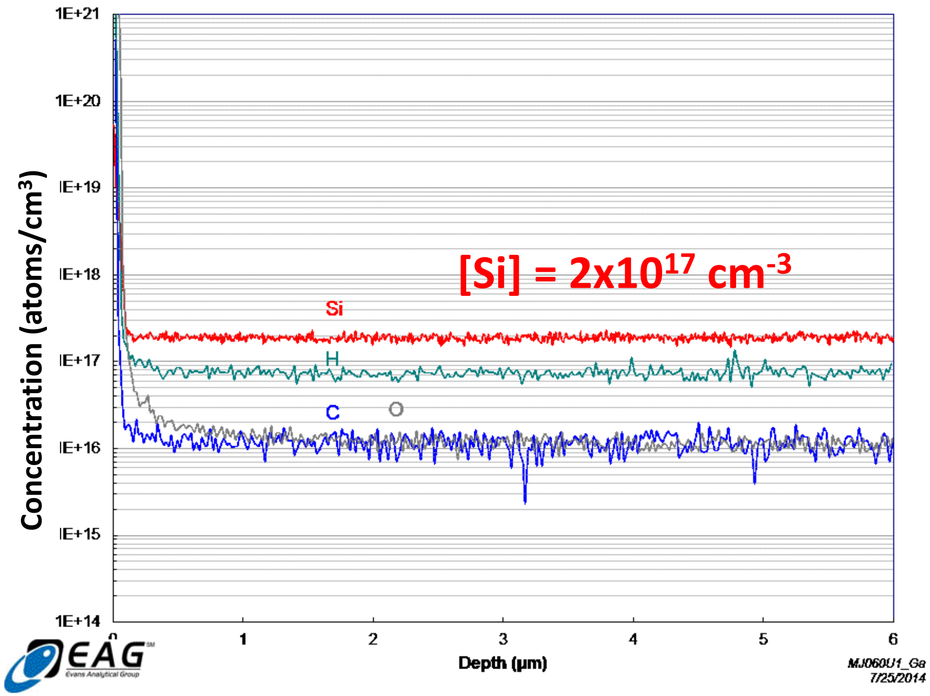

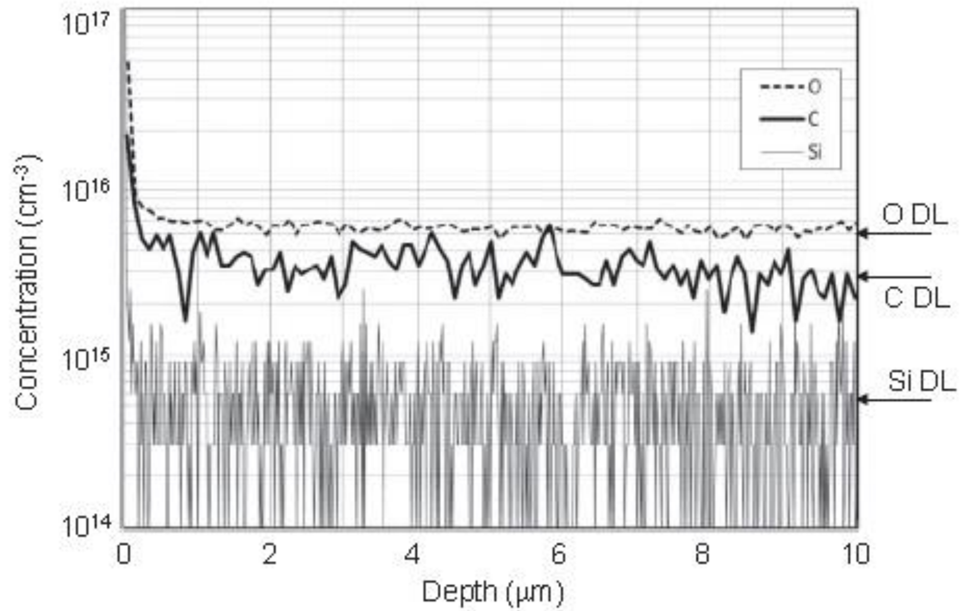

$n = 1\text{-}4\times10^{16}\ \mathrm{cm^{-3}}$
$\mu = 940\text{-}1100\ \mathrm{cm^2/Vs}$

unipress

J.A. Freitas Jr. Et al.,Journal of Crystal Growth 456 (2016) 113–120

$n = 2\times10^{14}\ \mathrm{cm^{-3}}$
$\mu = 1150\ \mathrm{cm^2/Vs}$

SCIOCS

H. Fujikura et al., Japanese Journal of Applied Physics 56, 085503 (2017)

GaN-based electronic devices

Thin n$^-$ GaN

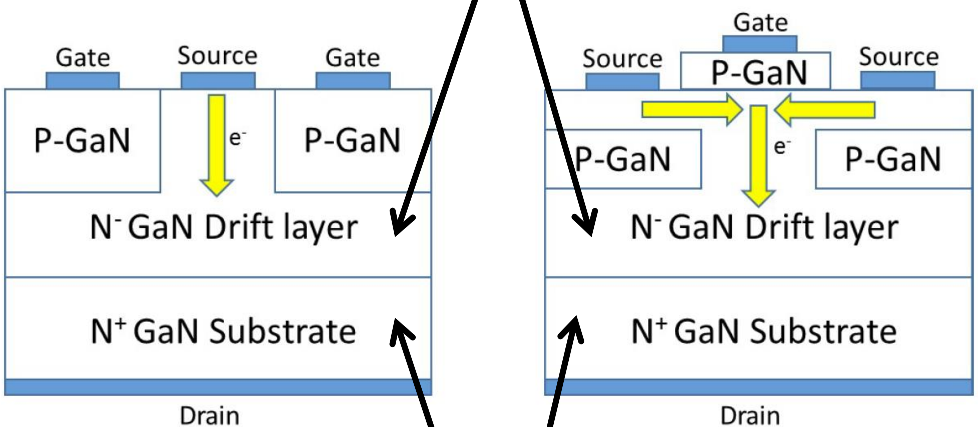

Figure 1: Two possible FET topologies. The arrows indicate the direction of electron flow.

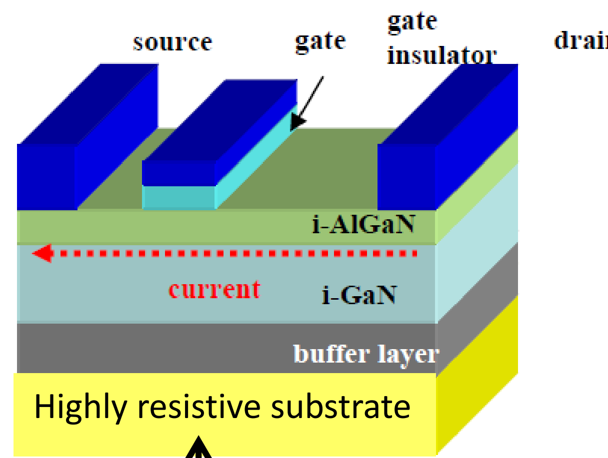

Bulk n$^+$ GaN

Bulk highly resistive GaN

Vertically operating

Laterally operating

Thin undoped HVPE-GaN

Thin HVPE-GaN layers

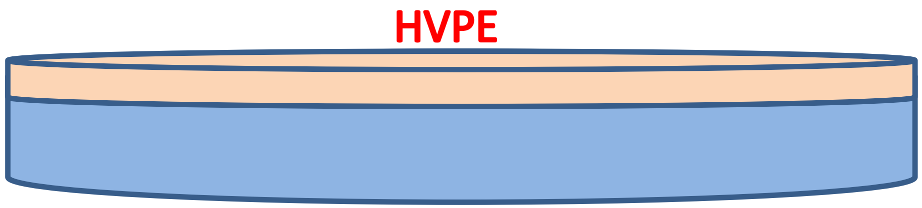

N^- GaN layer –
unintetionally doped (UID) GaN

N^+ GaN substrate

Defect selective etching in bases (KOH/NaOH) at 450°C

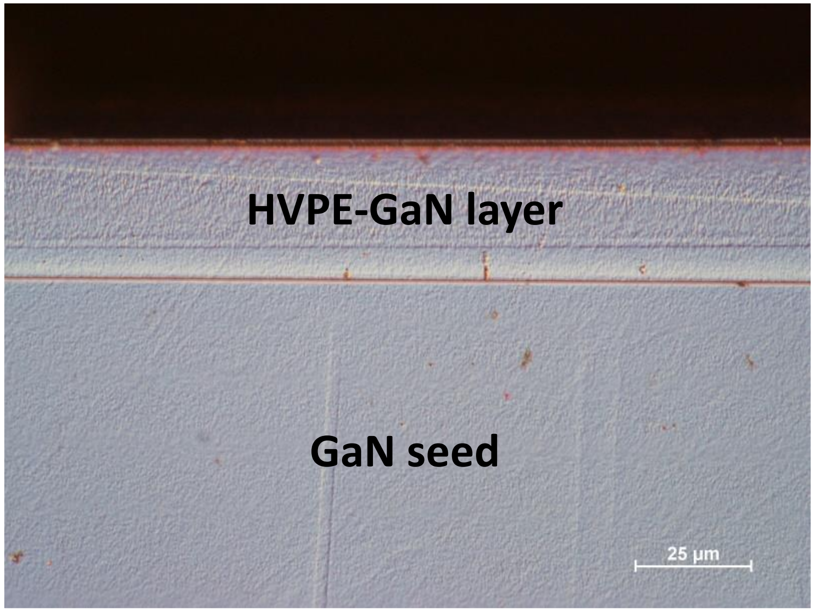

View of cross-section

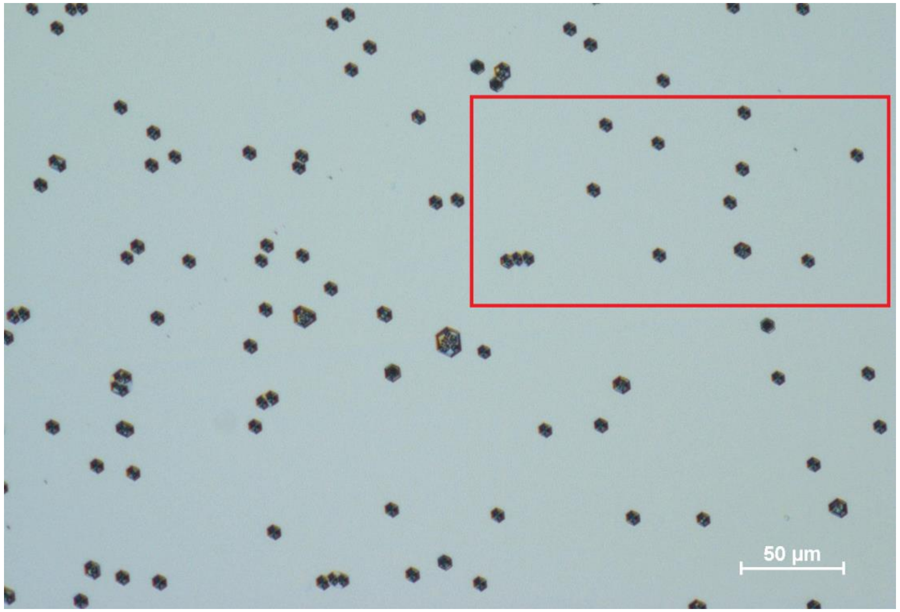

C-plane
Etch pit density: ~$5x10^4$ cm^{-2}

Thin HVPE-GaN layers - SIMS

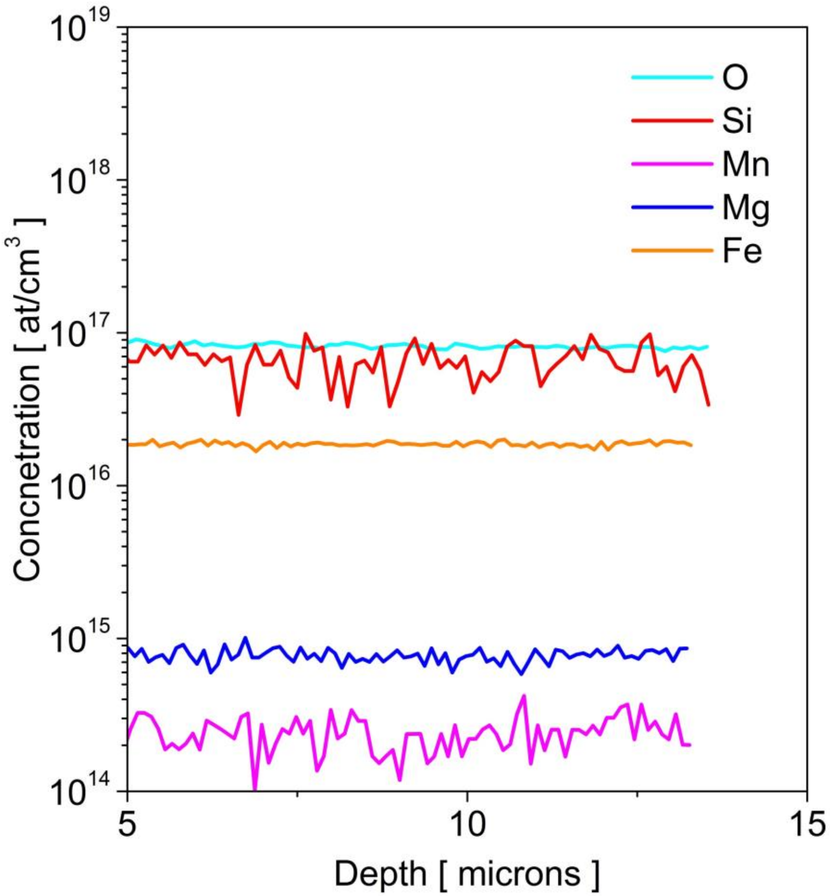

[O]	8e16 cm^{-3}
[Si]	6e16 cm^{-3}
[Fe]	2e16 cm^{-3}
[Mg]	8e14 cm^{-3}
[Mn]	3e14 cm^{-3}

Lower than SIMS background level:
[H] < 1e17 cm^{-3}
[C] < 2e16 cm^{-3}

Thin HVPE-GaN layers – E3 trap

E3:

1) N_{Ga} (D. Hasse et al., Appl. Phys. Lett. **69**, 2525 (1996).
2) Fe

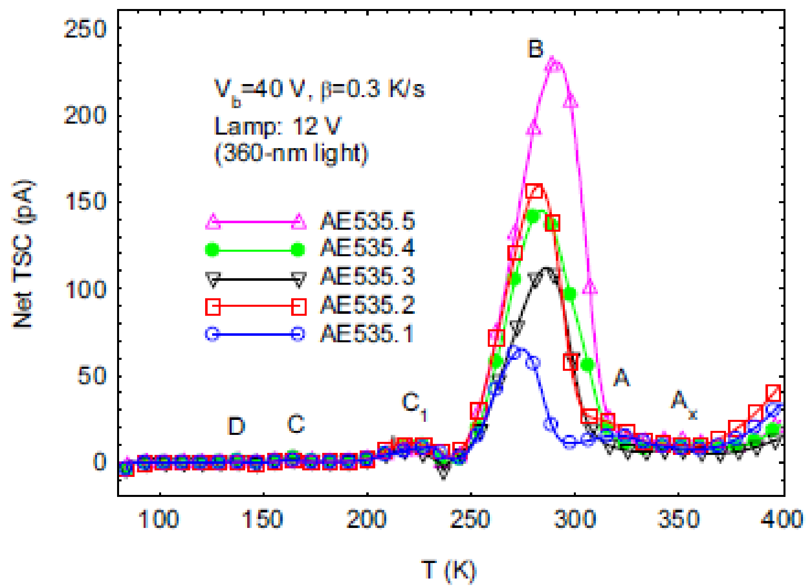

Figure 3 Net TSC (i.e., TSC-DC) spectra for the five samples.

7.5×10^{17} cm^{-3} < [Fe] < 2×10^{18} cm^{-3}

E_a = 0.56 to 0.60 eV

Z.-Q. Fang et al., Phys. Stat. Sol. (c) 5, No. 6 (2008)

Thin HVPE-GaN layers – E3 trap

UID GaN

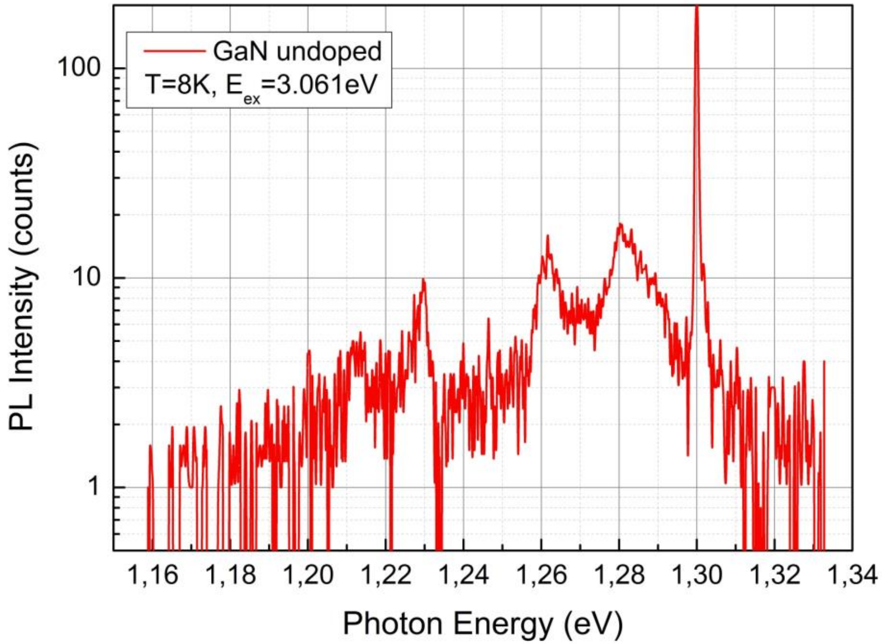

NIR PL for UID HVPE-GaN; sharp line representing Fe^{3+} in GaN visible at 1.3 eV ($^4T_1(G) \rightarrow {}^6A_1(S)$ transition)

[Fe] ~2×10^{16} cm^{-3}

Bulk n^+ GaN

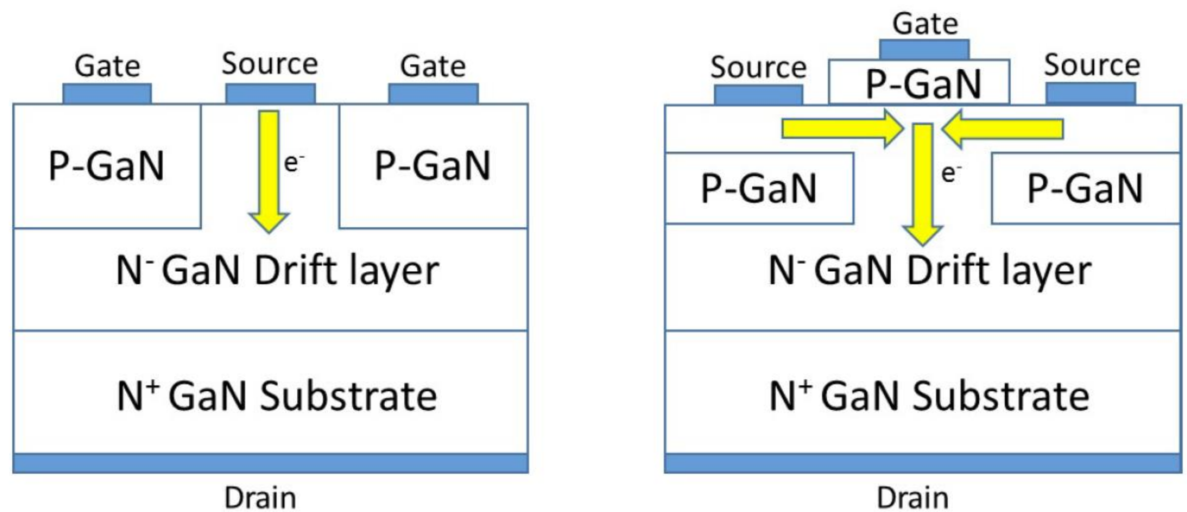

Figure 1: Two possible FET topologies. The arrows indicate the direction of electron flow.

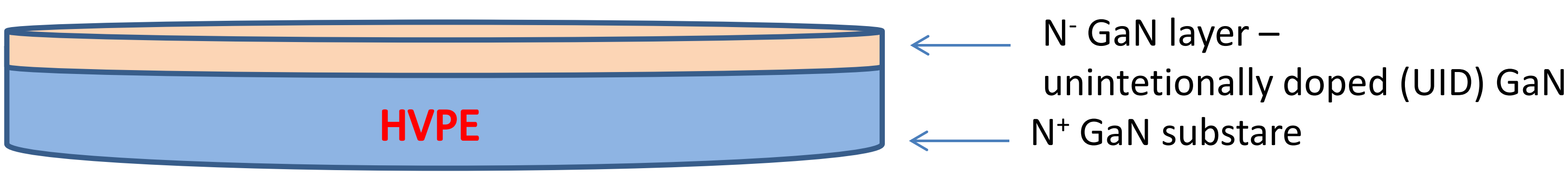

N-type doping

Doping with Si and Ge

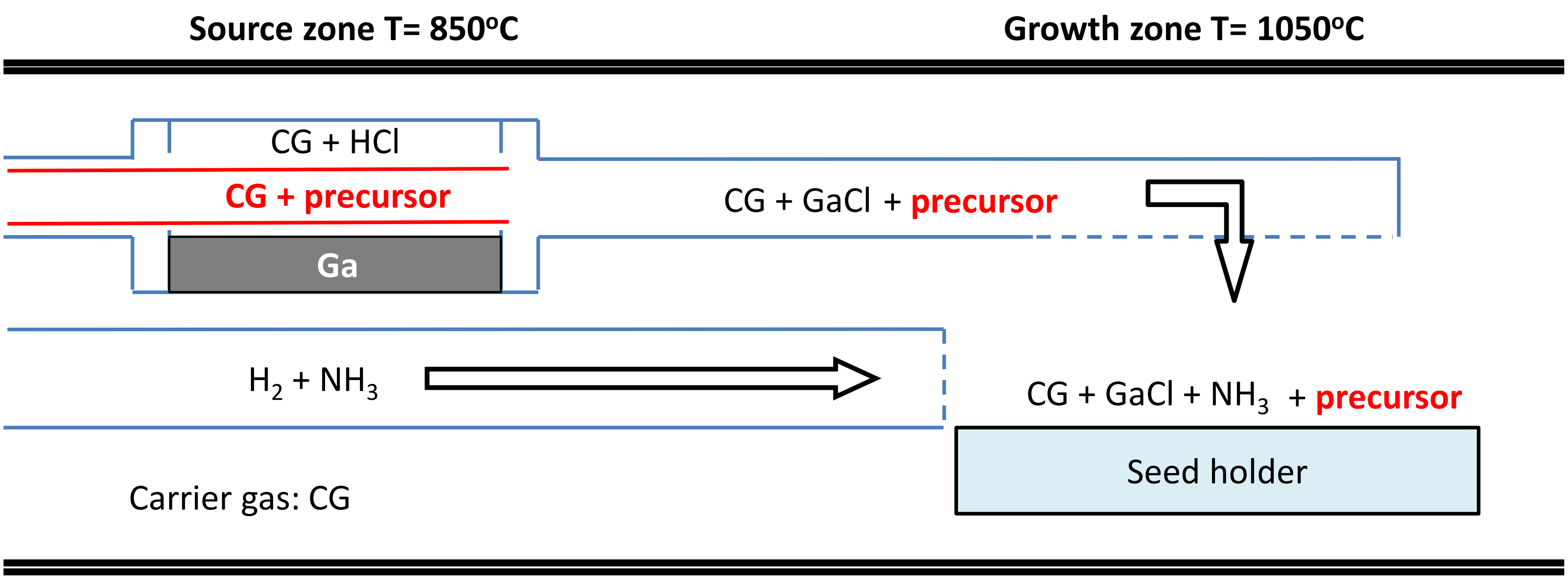

Dopant	Precursor
Si	H_2SiCl_2
Ge	$GeCl_4$

Free carrier uniformity on c-plane

GaN:Si

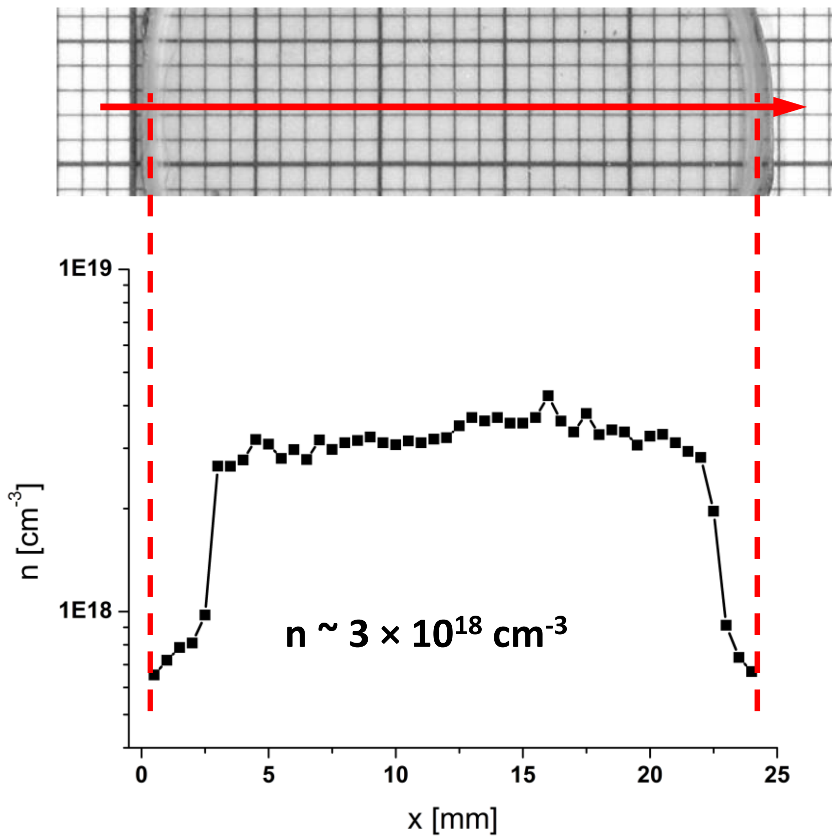

GaN:Ge

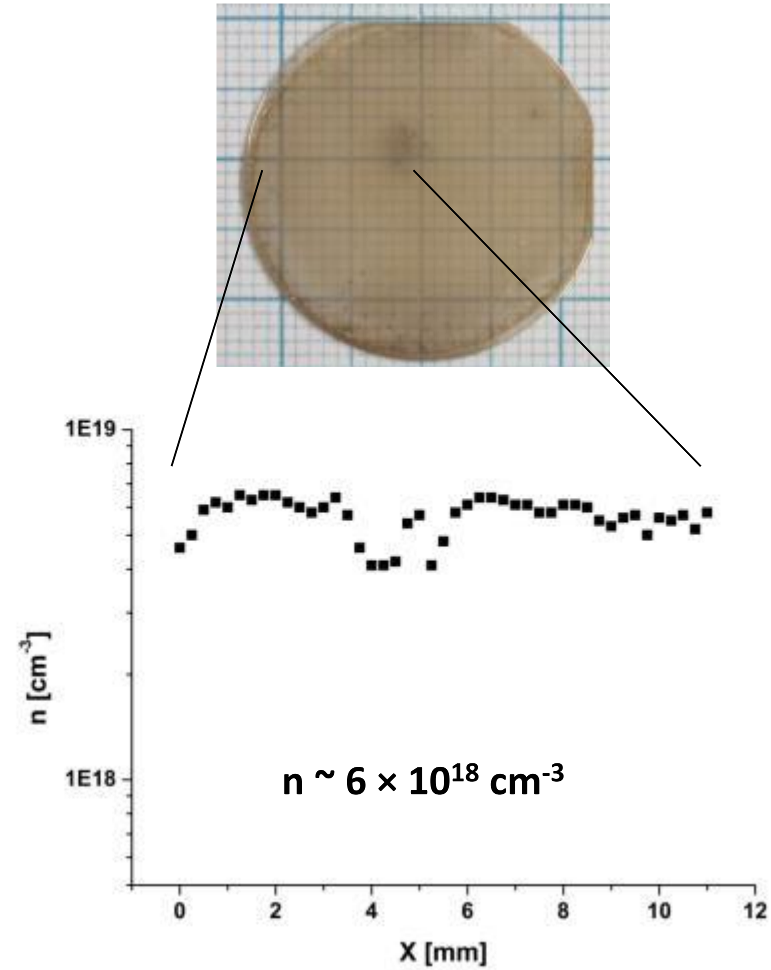

Free carrier uniformity along c-axis

GaN:Si

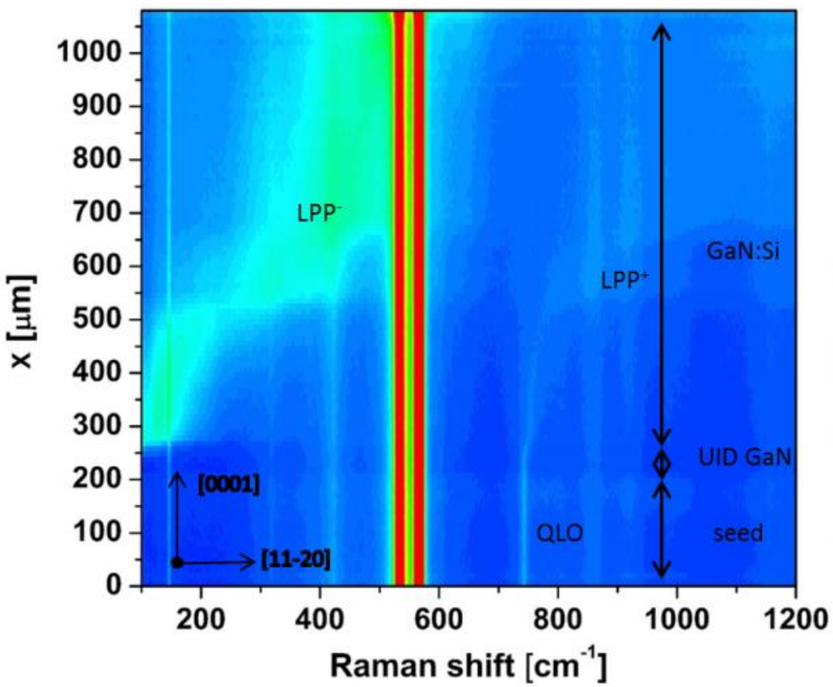

GaN:Ge

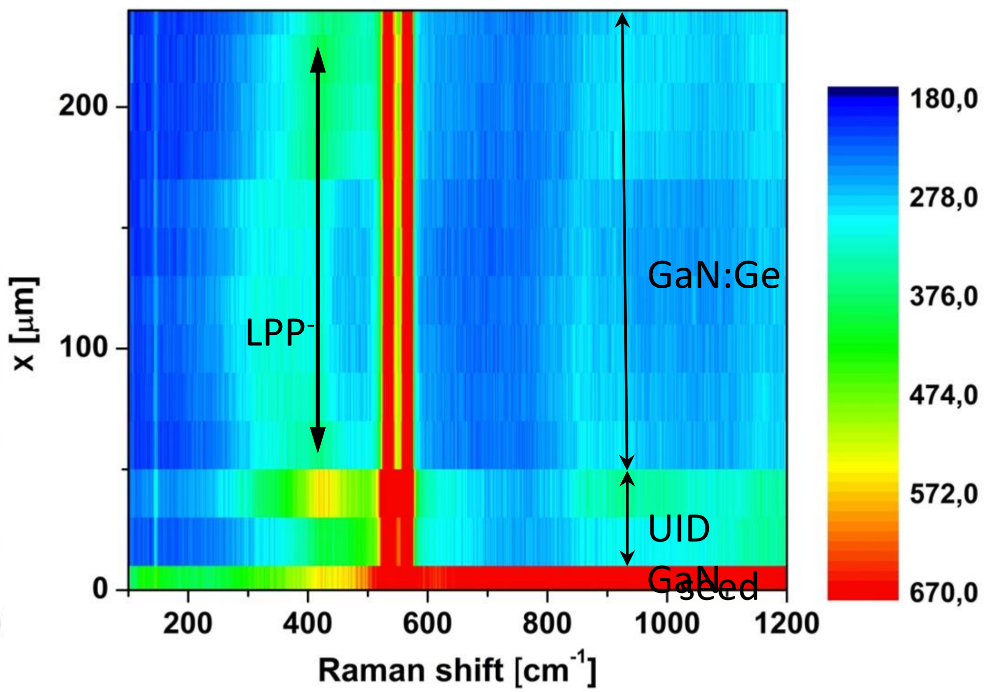

Free carrier concentration vs Si concentration

GaN:Si

H_2SiCl_2 flow [ml min^{-1}]	[Si] SIMS [cm^{-3}]		n (Hall) [cm^{-3}]
0.8	6E19	>	3E18
0.04	3E19	>	4E18

GaN:Ge

nGe/nGa [%]	[Ge] (SIMS) [cm^{-3}]		n(Hall) [cm^{-3}]	n(Raman) [cm^{-3}]	N_D-N_A (CV) [cm^{-3}]
0.0660	7E+19	≈	5.07E+19	6.4E+19	1E+19
0.0165	6E+18	≈	4.6E+18	5E+18	4E+18
0.0116	2E+18	≈	2.8E+18	1.8E+18	2,5E+18

Low-temperature PL

GaN:Si

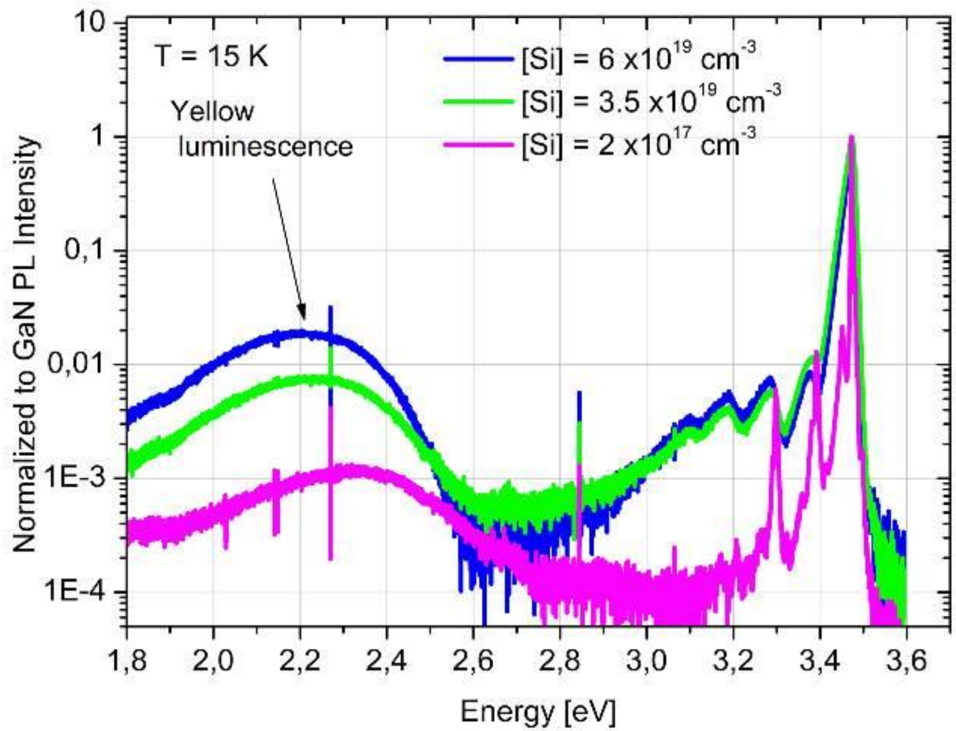

M. Iwinska et al., J. Cryst. Growth 456, 91–96, (2016)

GaN:Ge

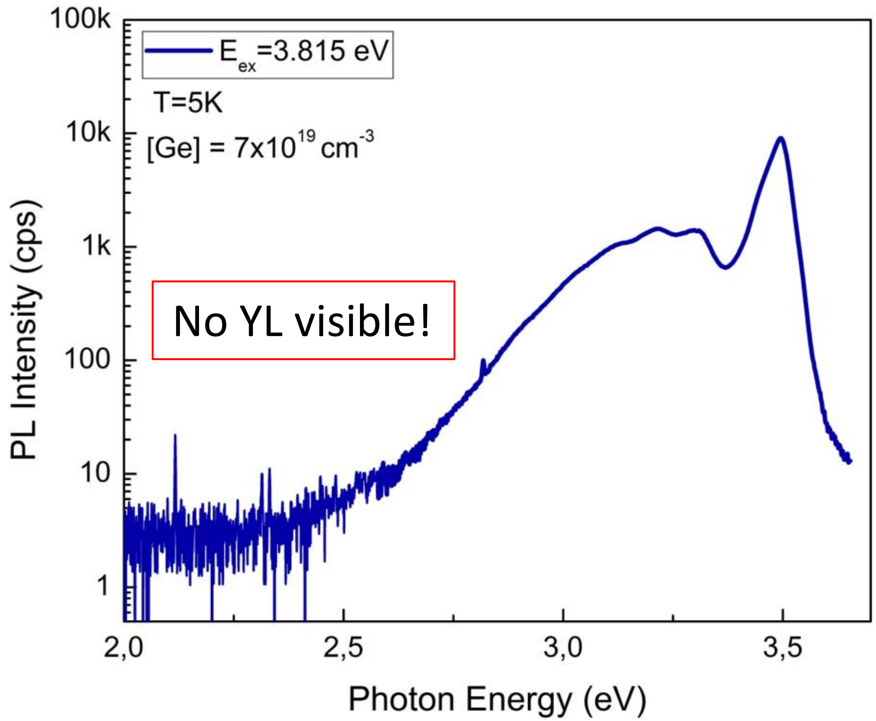

M. Iwinska et al., J. Cryst. Growth 480 (2017) 102–107

Yellow luminescence in GaN

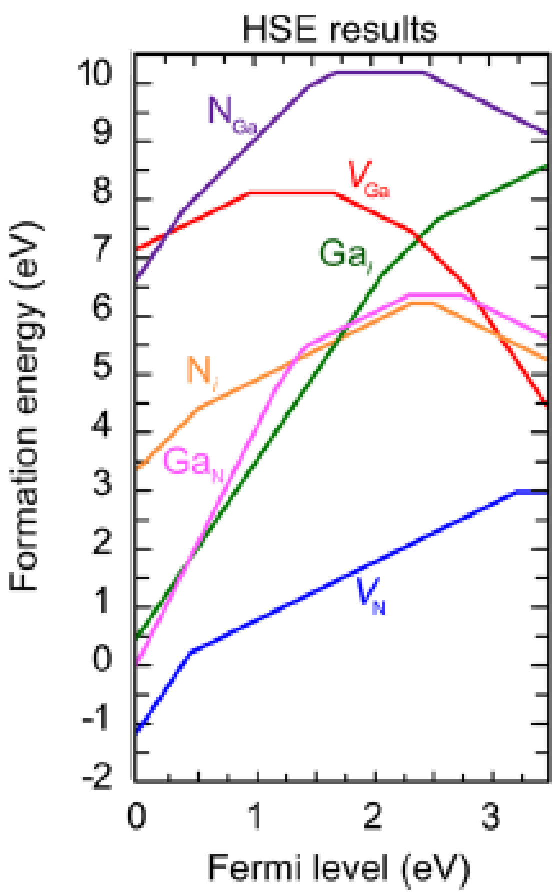

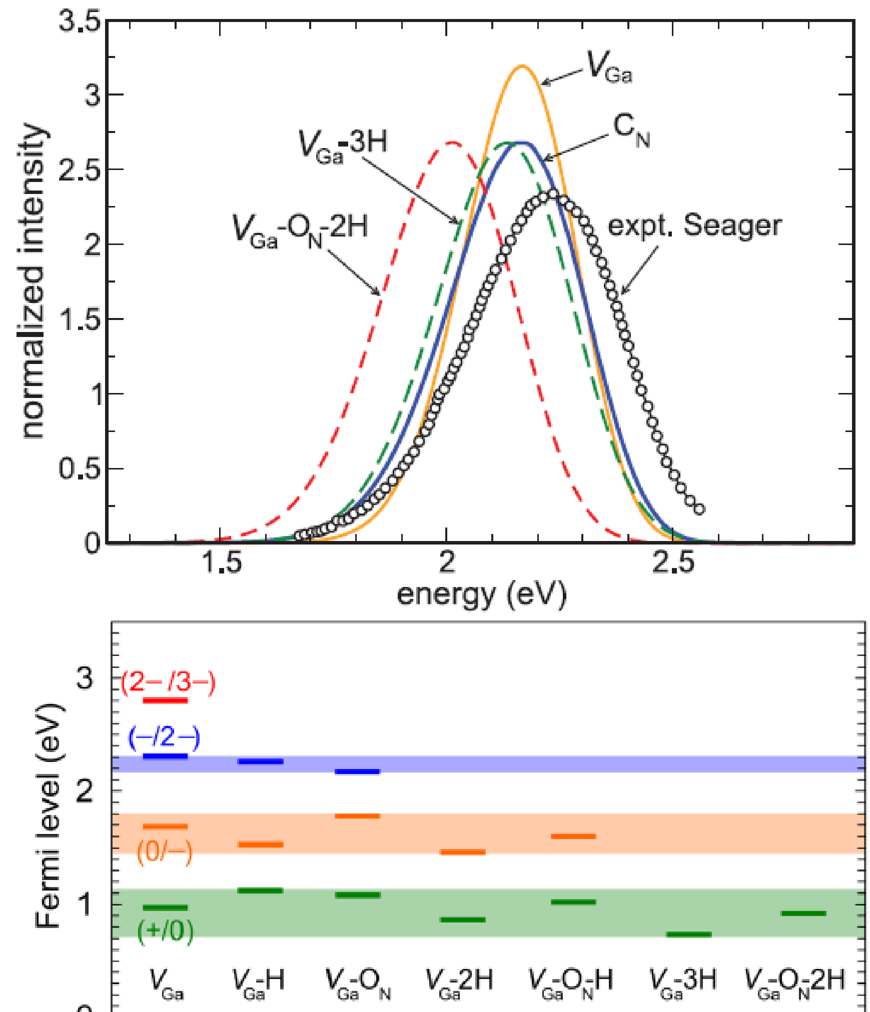

JL Lyons and CG Van de Walle,
npj Computational Materials 3 (2017) 12

John L. Lyons et al., Phys. Status Solidi B 252, No. 5 (2015)

Challenges with Si and Ge doping

GaN:Si

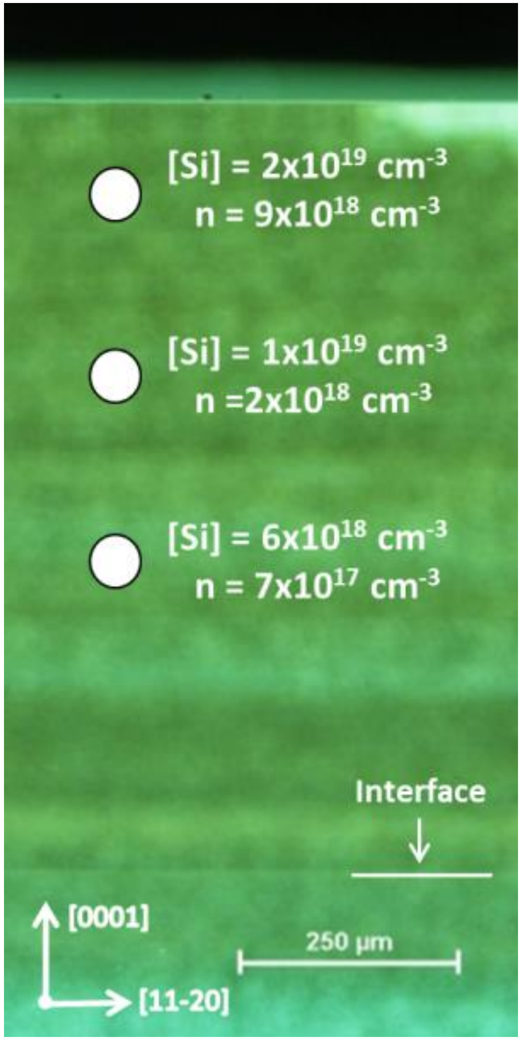

GaN:Ge

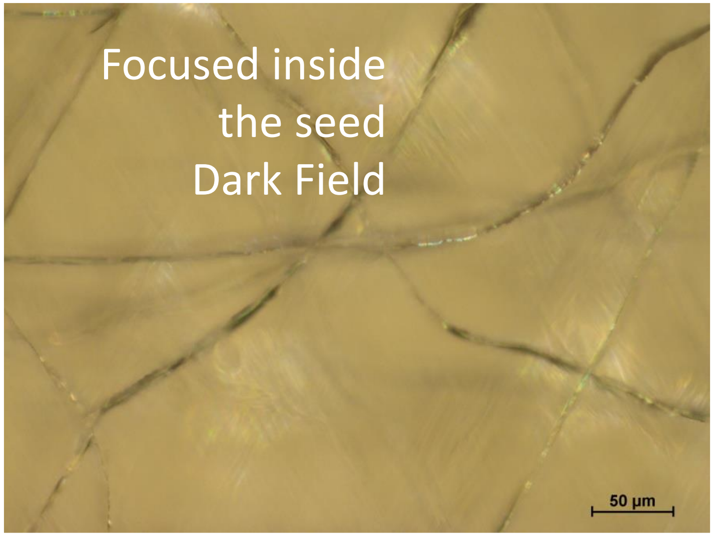

Si and Ge doping - summary

Si-doped	Ge doped
Thick layers (up to 1.5 mm)	Thin layers (~300 µm)
Not all Si electrically active	Free carrier concentration at the same level as [Ge]
Yellow luminescence – point defects present	No yellow luminescence
Uniform free carrier distribution on c-plane	Uniform free carrier distribution on c-plane
Silicon and free carrier gradient along c-axis	Uniform free carrier distribution along c-axis

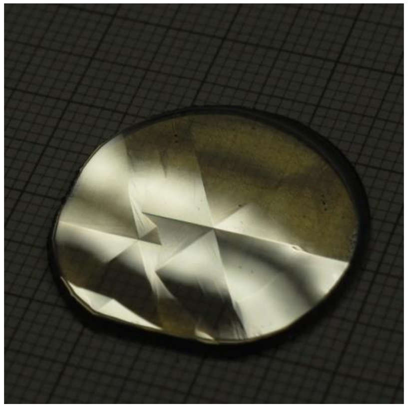

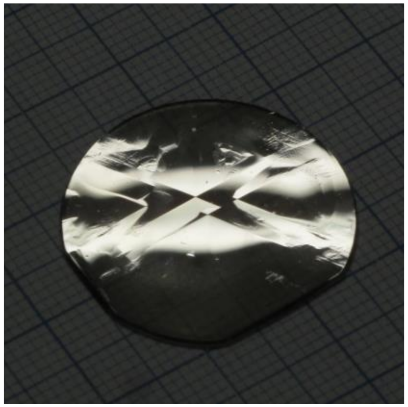

Highly resistive GaN
GaN:Fe

Fe doping in HVPE

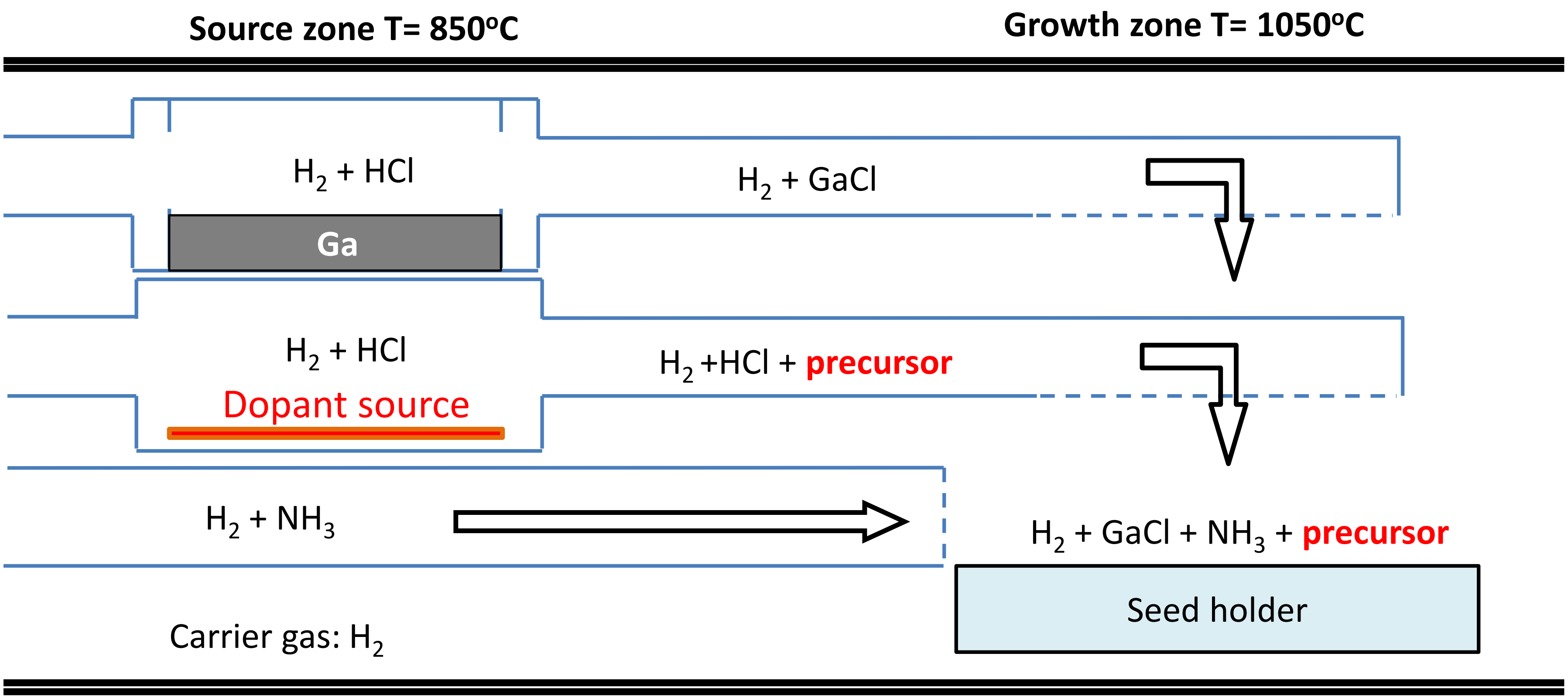

Dopant	Precursor
Fe	$FeCl_2/FeCl_3$

Fe-doped GaN

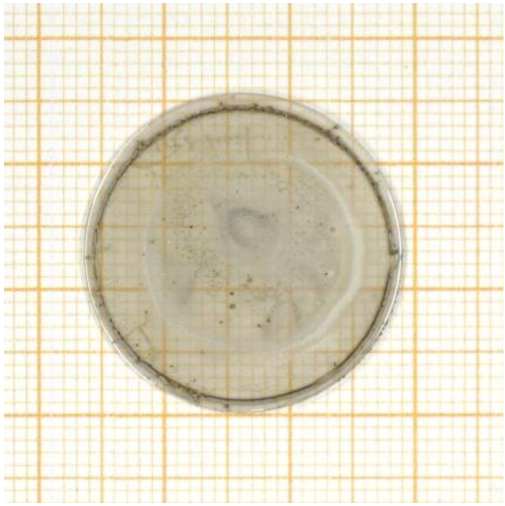

Layer thicknes: 300-600 µm

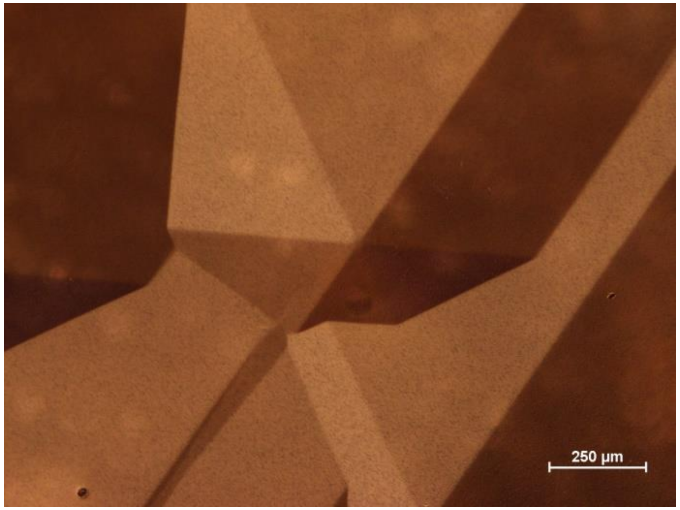

	Seed (CMP)	GaN:Fe (as grown)
FWHMx [arcsec]	30	30
FWHMy [arcsec]	32	31
Rx [m]	24.6	21
Ry [m]	37.2	15.1

[Si]	9e16 - 3e17 cm^{-3}
[Fe]	**6e16 - 3e17 cm^{-3}**
[Mg]	8e14 – 1e15 cm^{-3}
[Mn]	5e14 - 4e15 cm^{-3}

Lower than SIMS background level:
[O] < 1e17 cm^{-3}
[H] < 1e17 cm^{-3}
[C] < 2e16 cm^{-3}
[Ge] < 1e16 cm^{-3}

Fe-doped GaN – electrical properties (II)

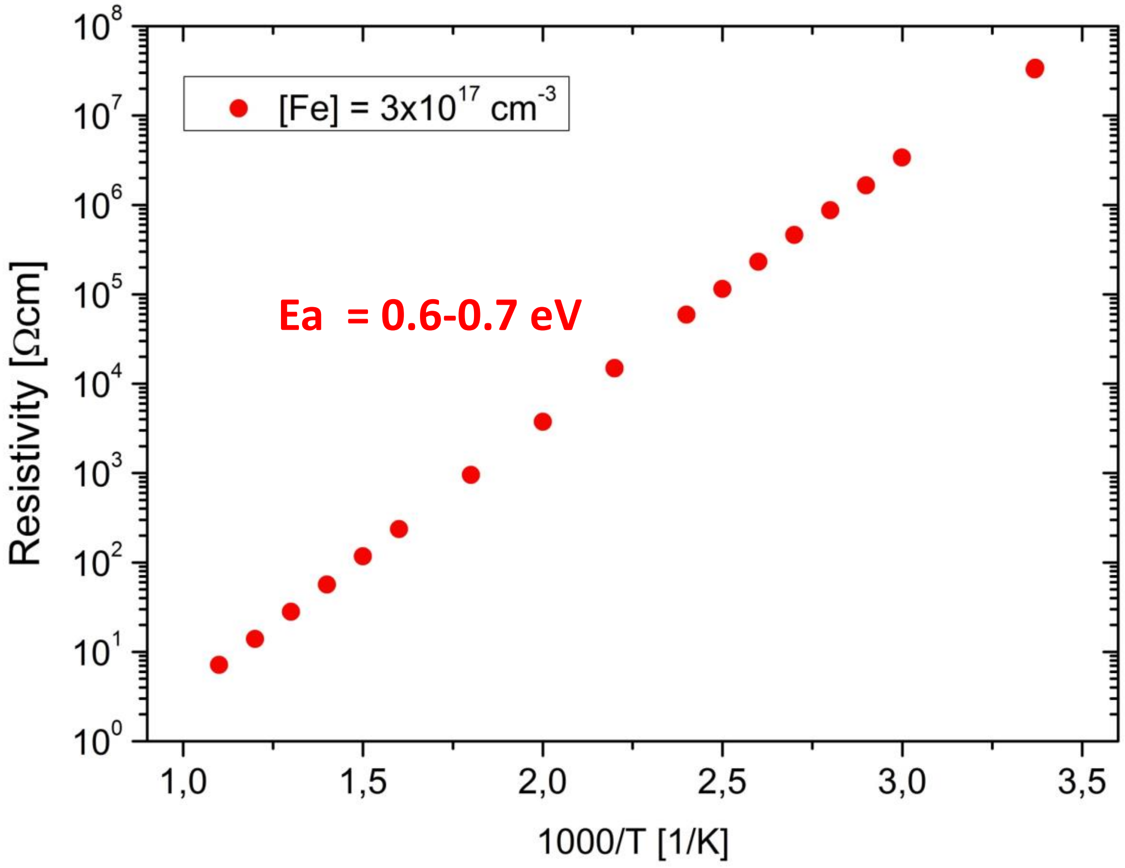

Fe-doped GaN – electrical properties (I)

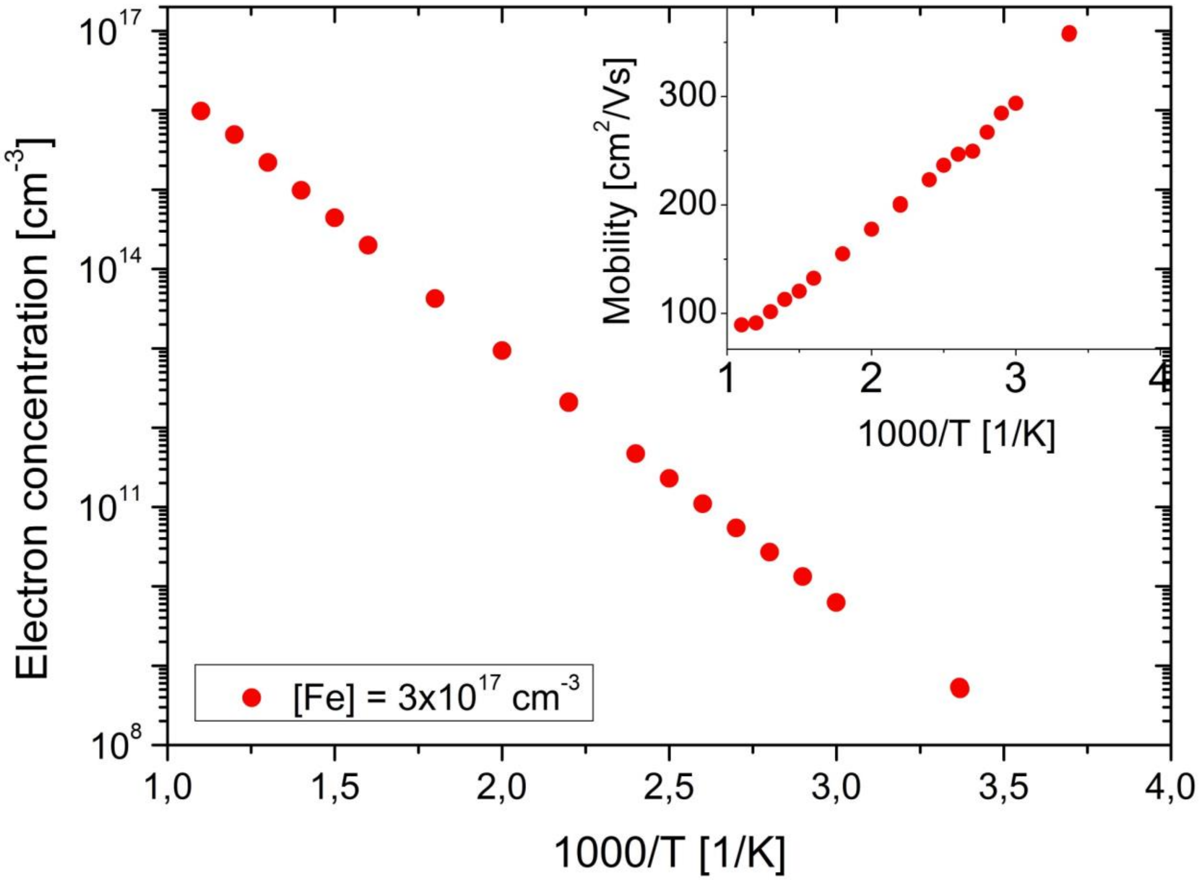

GaN:Mn

Mn in GaN

Position of the $Mn^{3+/2+}$ and $Mn^{3+/4+}$ levels determined experimentally and theoretically, respectively.

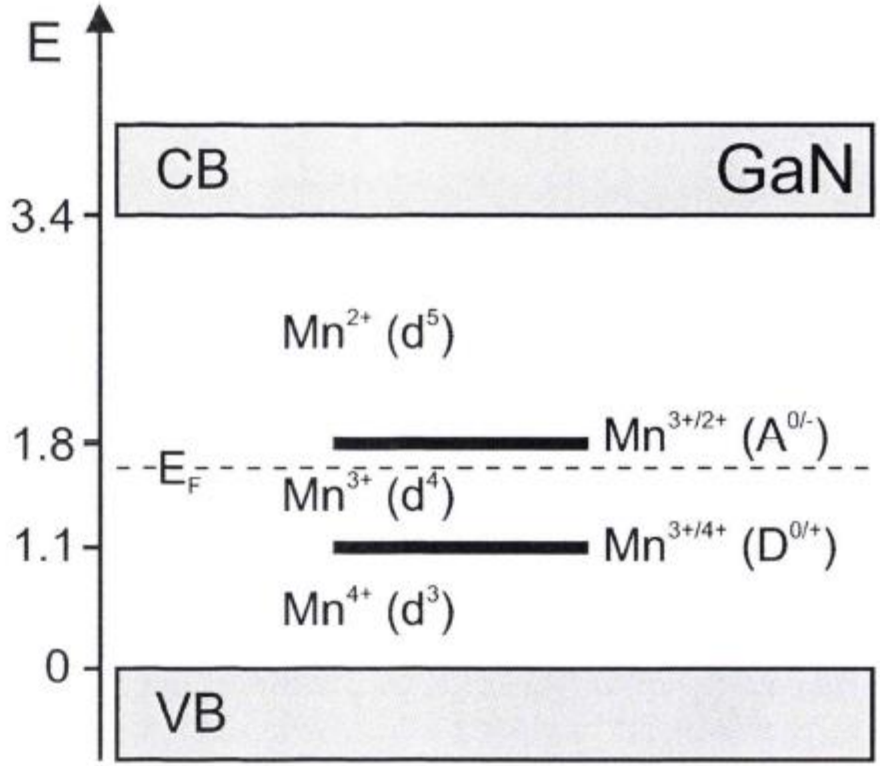

E. Malguth, PhD Thesis, Technische Universitat Berlin, Germany (February 2008)
U. Gerstmann et al., Phys. Rev. B 63(7): 075204 (2001).
T. Graf et al., Appl. Phys. Lett. 81(27): 5159— 5161 (2002).

Mn doping in HVPE

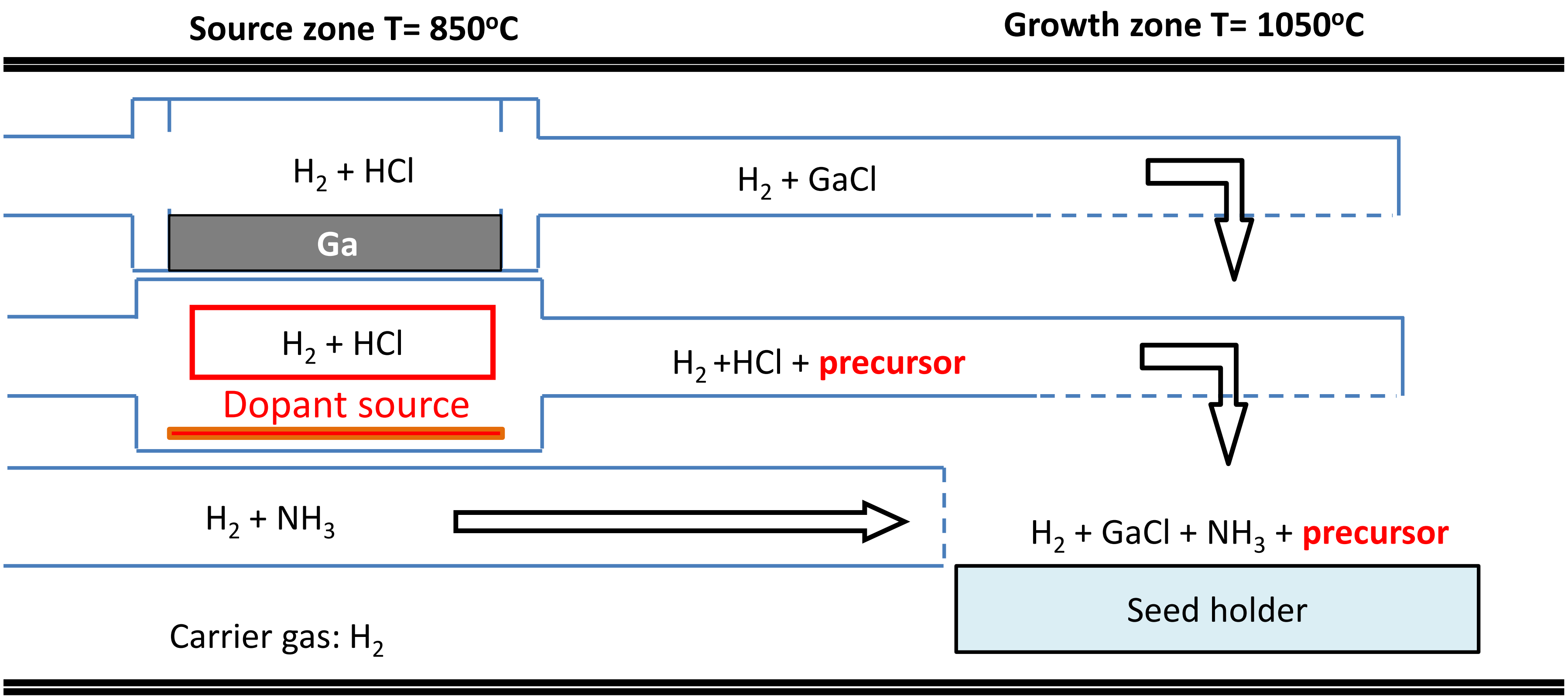

Dopant	Precursor
Mn	$MnCl_2/MnCl_3$

Mn-doped GaN

	A	B	C
HCl [ml/min]	48	48	48
NH_3 [ml/min]	960	960	960
HCl over Mn [ml/min]	0	0	0.1
H_2 over Mn [ml/min]	300	600	300
Time [h]	~3	3	4
Growth rate [µm/h]	220	165	218
Seed thickness [µm]	423	482	540
Layer thickness [µm]	662	496	656

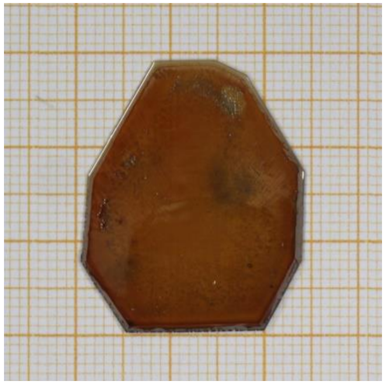

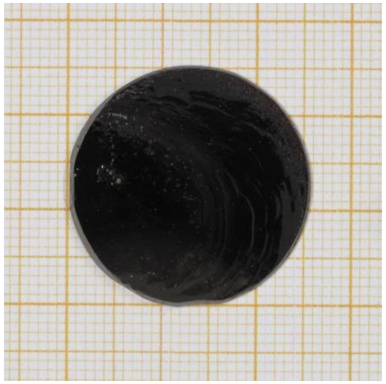

Mn-doped GaN

	A	B	C
HCl [ml/min]	48	48	48
NH_3 [ml/min]	960	960	960
HCl over Mn [ml/min]	0	0	0.1
H_2 over Mn [ml/min]	300	600	300
[Mn] SIMS [cm^{-3}]	$1x10^{16}$	$1x10^{17}$	$4x10^{19}$

Seed (CMP)/GaN:Mn (as grown)			
FWHM(002) [arcsec]	83/72	36/234	-

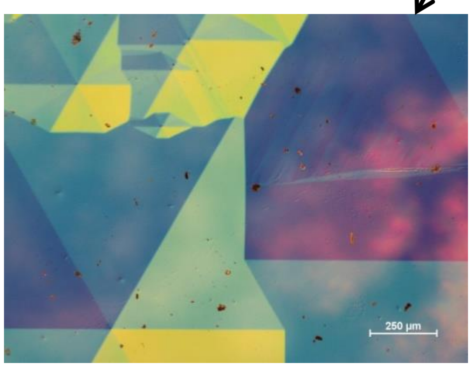

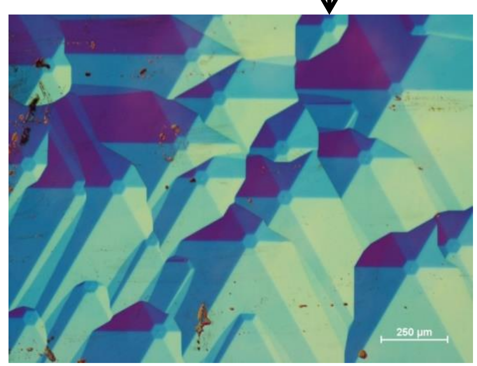

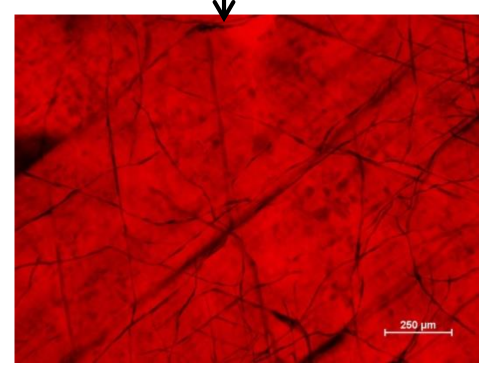

Mn-doped GaN – electrical properties

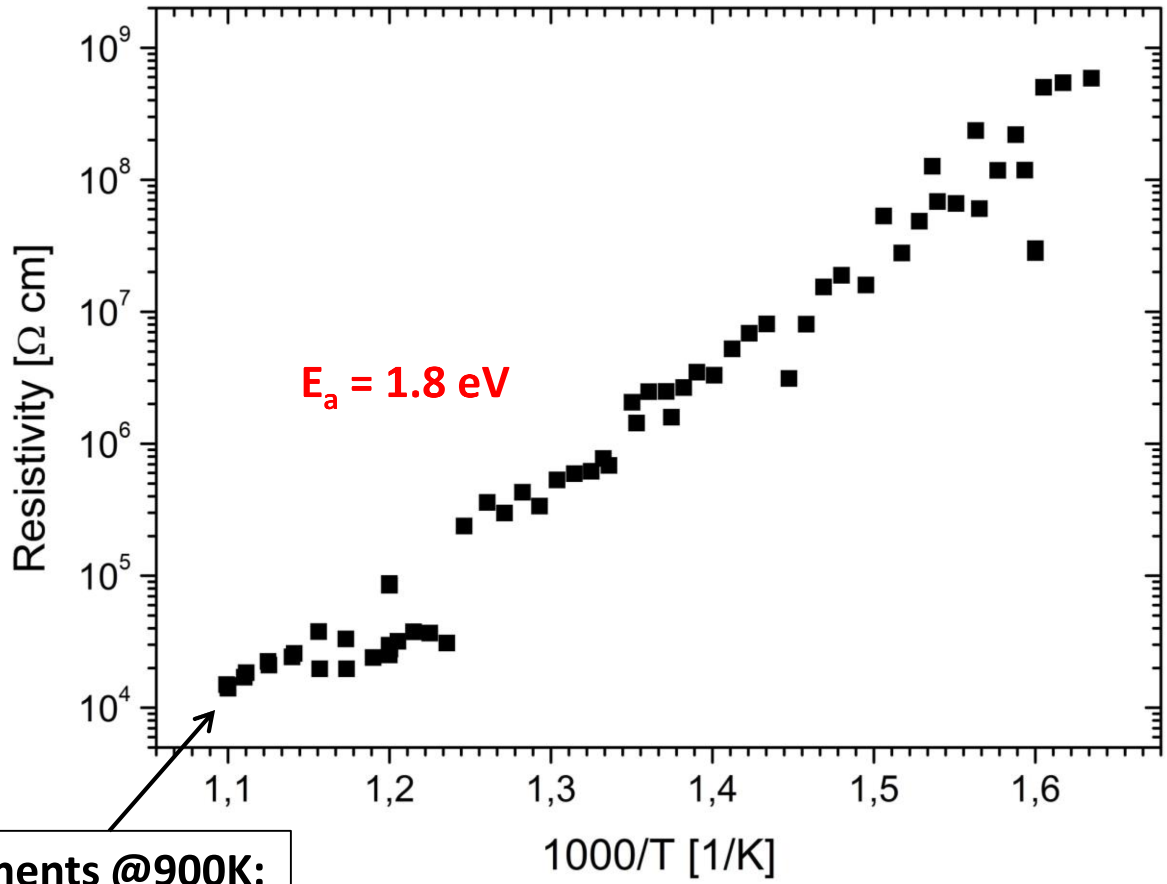

Hall measurements @900K:
n = 3×10^{13} cm^{-3}
μ = 12 cm^2/Vs

GaN:C

C in GaN

PHYSICAL REVIEW B **89**, 035204 (2014)

Effects of carbon on the electrical and optical properties of InN, GaN, and AlN

J. L. Lyons,* A. Janotti, and C. G. Van de Walle

C_N is a deep acceptor with the (0/–) transition level at 0.90 eV above the VBM

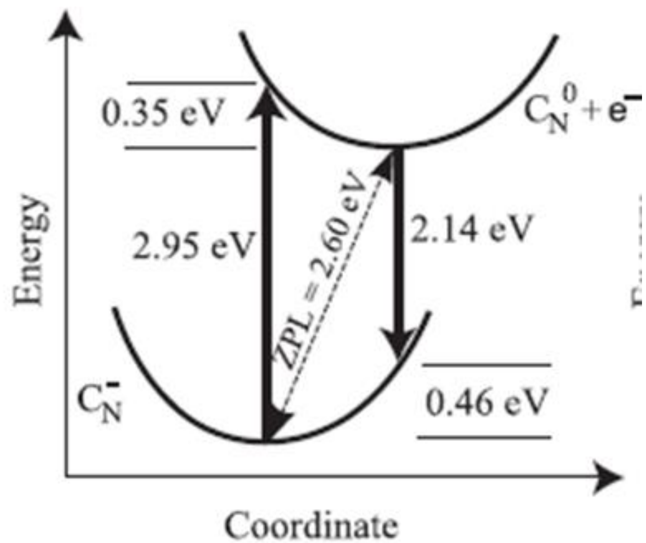

FIG. 3. Configuration-coordinate diagrams for the C_N impurity in GaN. (a) If electrons in the conduction band recombine with $C_{NN}^{0\,0}$, the emission associated with the $C_N^0 + e^- \rightarrow C_N^-$ transition is predicted to occur with a peak at 2.14 eV.

C doping in HVPE

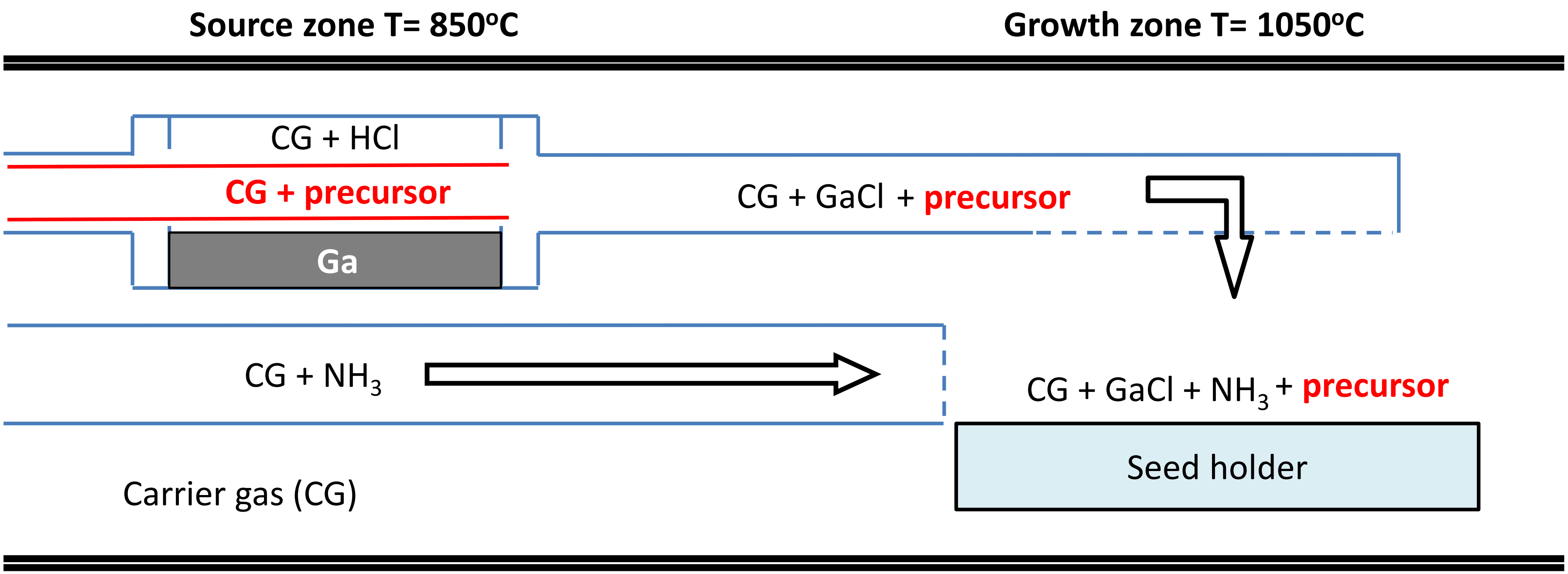

Dopant	Precursor
C	CH_4

C-doped GaN – electrical properties

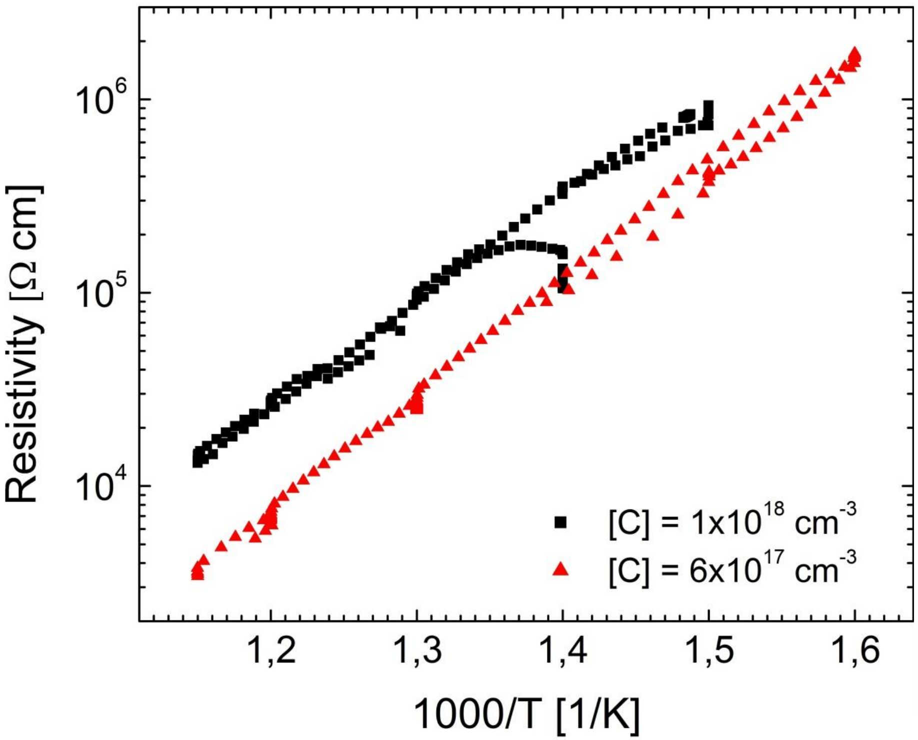

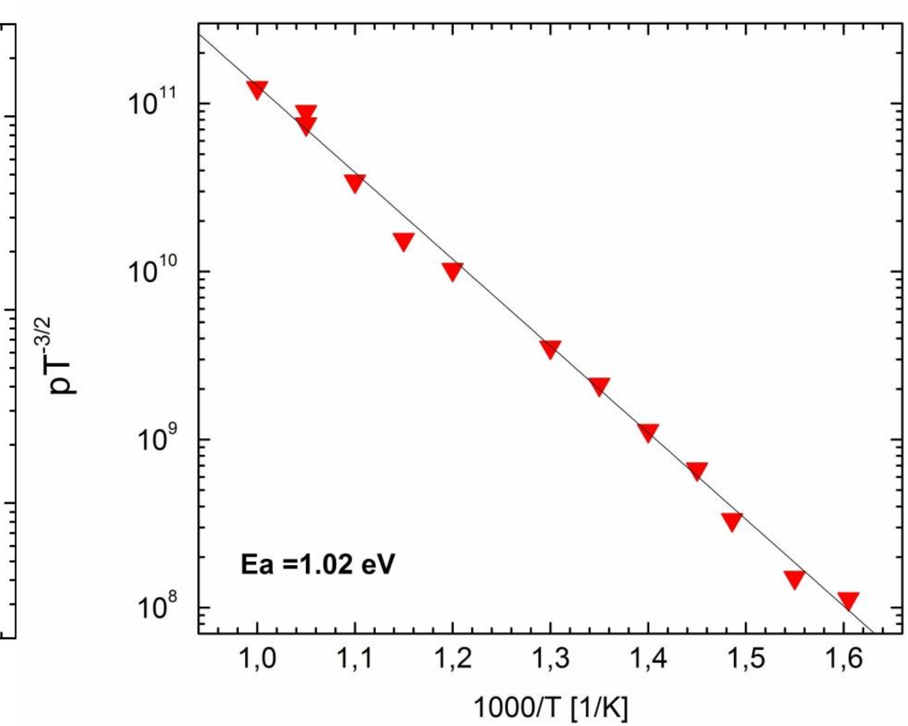

Activation energy ~1 eV

M. Iwinska et al., Applied Physics Express 10, 011003 (2017)

C-doped GaN – EPR

HVPE-GaN:C

TABLE I. Carbon impurity concentrations measured by secondary-ion mass spectrometry and spin densities by electron paramagnetic resonance before and after illumination with 400 nm LED.

Sample	SIMS [C], 10^{18} cm^{-3}	EPR spin density before illumination, 10^{18} cm^{-3}	EPR spin density after illumination, 10^{18} cm^{-3}
A	6	0.2	1.5
B	6	0.2	1.5
C	10	0.1	1.0

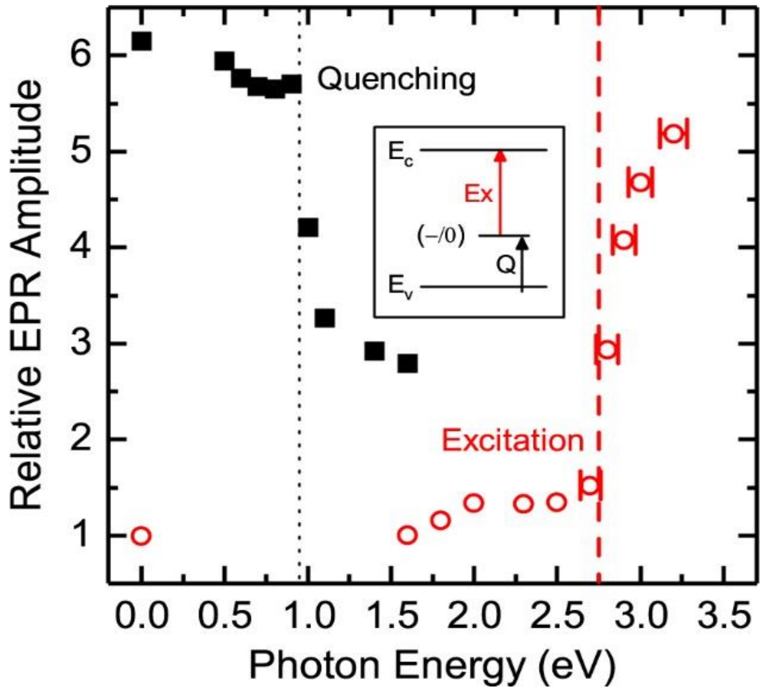

acceptor level 0.95 eV above the VBM

Willoughby et al. J. Appl. Phys. 123, 161547 (2018)

Fe, Mn, or C for high resistivity?

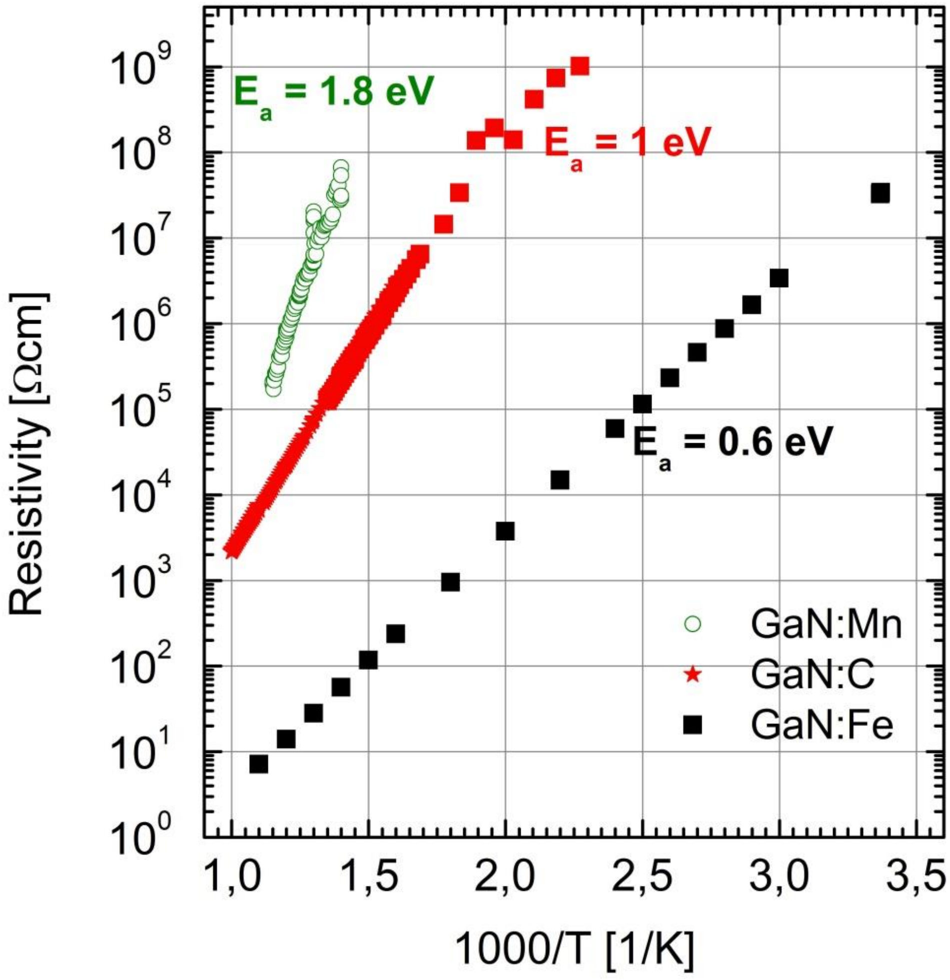

unipress

This research was supported by ONR Global through program NICOP: N62909-17-1-2004

and by Polish National Science Centre (NCN) through OPUS project 2017/25/B/ST5/02897

National Science Centre
Poland

Thank you for your attention!